Catal Lett (2012) 142:267–274
DOI 10.1007/s10562-011-0757-1

Aqueous-Phase Hydrogenolysis of Glycerol to 1,3-propanediol Over Pt-$H_4SiW_{12}O_{40}/SiO_2$

Shanhui Zhu · Yulei Zhu · Shunli Hao · Lungang Chen · Bin Zhang · Yongwang Li

Received: 30 September 2011 / Accepted: 5 December 2011 / Published online: 20 December 2011

Abstract Hydrogenolysis of glycerol to 1,3-propanediol in aqueous-phase was investigated over Pt-$H_4SiW_{12}O_{40}/SiO_2$ bi-functional catalysts with different $H_4SiW_{12}O_{40}$ (HSiW) loading. Among them, Pt-15HSiW/SiO_2 showed superior performance due to the good dispersion of Pt and appropriate acidity. It is found that Brønsted acid sites facilitate to produce 1,3-PDO selectively confirmed by Py-IR. The effects of weight hourly space velocity, reaction temperature and hydrogen pressure were also examined. The optimized Pt-HSiW/SiO_2 catalyst showed a 31.4% yield of 1,3-propanediol with glycerol conversion of 81.2% at 200 °C and 6 MPa.

Keywords Glycerol · Hydrogenolysis · 1,3-propanediol · Silicotungstic acid

1 Introduction

The conversion and utilization of renewable biomass provide a facile route to alleviate the shortage of fossil fuels and reduce the CO_2 emission [1–4]. In this context, biomass-derived polyols emerge as promising building blocks for liquid fuels and valuable commodity chemicals [5–10]. Among them, glycerol is especially attractive because it can be converted to a wide range of value-added chemicals by catalytic processes such as reforming, oxidation, dehydration, esterification, etherification, hydrogenolysis, polymerization and so on [1, 6, 9, 11]. In addition, glycerol is a by-product in a large amount from the production of biodiesel by transesterification of plant and animal oils with methanol [1, 6]. Therefore, it is essential for the sustainable development of biodiesel industry to effectively utilize the renewable glycerol.

Hydrogenolysis of glycerol to 1,2-propanediol (1,2-PDO) and 1,3-propanediol (1,3-PDO) is a noticeable pathway for the production of renewable value-added chemicals. 1,3-PDO owes much higher economical value than 1,2-PDO, in particular, as an important monomer in the synthesis of polyester fibers [1, 6, 11]. Industrial production of 1,3-PDO is currently based on chemical synthesis via hydration of acrolein or hydroformylation of ethylene oxide [12]. In comparison with petroleum-derived acrolein and ethylene oxide, glycerol is not only renewable, but also structurally analogous to 1,3-PDO. These features render glycerol to be preferential feedstorks, in terms of sustainability and energy efficiency, for the synthesis of 1,3-PDO by catalytic hydrogenolysis.

Conversion of glycerol to 1,2-PDO has been extensively studied in recent years, and high yields have been obtained in previous reports [8, 9, 13–22]. In contrast, direct hydrogenolysis of glycerol to 1,3-PDO is still a challenge. Several patents and papers have disclosed 1,3-PDO production by the catalytic hydrogenolysis of glycerol in the presence of homogeneous or heterogeneous catalysts. Che [23] found that glycerol can be hydrogenolyzed to 1,3-PDO

S. Zhu · Y. Zhu (✉) · L. Chen · B. Zhang · Y. Li
State Key Laboratory of Coal Conversion, Institute of Coal Chemistry, Chinese Academy of Sciences, 030001 Taiyuan, People's Republic of China
e-mail: zhuyulei@sxicc.ac.cn

S. Zhu · L. Chen · B. Zhang
Graduate University of Chinese Academy of Sciences, 100039 Beijing, People's Republic of China

S. Hao
Synfuels China Co. Ltd, 030032 Taiyuan, People's Republic of China

and 1,2-PDO in yields of 21 and 23%, respectively, at 200 °C and 32 MPa syngas in 1-methyl-2-pyrolidinone on a homogeneous rhodium complexes catalyst $Rh(CO)_2$(acac) with H_2WO_4 as a promoter. Chaminand et al. [24] reported that hydrogenolysis of glycerol to 1,3-PDO on Rh/SiO_2 catalyst achieved 4% yield in the presence of H_2WO_4 at 200 °C and 8.0 MPa. Kurosaka et al. [25] obtained 24% yield of 1,3-PDO from glycerol in 1,3-dimethyl-2-imidazolidinone over Pt/WO_3/ZrO_2 at 170 °C and 8.0 MPa. Tomishige et al. [26, 27] reported that the yield of 1,3-PDO reached 38% over Ir-ReO_x/SiO_2 catalyst with H_2SO_4 as an additive in a batch reactor. Additionally, other effective hydrogenolysis processes that have been reported recently employed Rh-ReO_x/SiO_2 [8], Pt/WO_3/TiO_2/SiO_2 [28], bimetallic Pt–Re [29], and Pt/WO_3/ZrO_2 [30] as heterogeneous catalysts.

These previous efforts have demonstrated the feasibility of the direct hydrogenolysis route in the synthesis of 1,3-PDO. However, these studies also remain several problems. Most of the previous studies have been performed in organic solvent, which will greatly reduce the environmental and economical viability. Another disadvantage arises from use of liquid acids, e.g., H_2WO_4, H_2SO_4, which will cause problems in terms of catalyst separation, reactor corrosion and environmental protection. Furthermore, the previous processes are mainly discontinuous, leading to difficulty in catalyst and product separation.

The development of a novel catalyst system for this environmentally friendly reaction has attracted considerable attention. Alhanash et al. [17] reported that 5% Rh/$Cs_{2.5}H_{0.5}[PW_{12}O_{40}]$ catalyst gave 7.1% selectivity of 1,3-PDO in liquid phase. We have previously investigated vapor-phase hydrogenolysis of glycerol over Cu-HSiW/SiO_2 without employing solvent in a fixed-bed reactor [31]. Replacement of liquid acid catalysts with supported HSiW would remove energy-consuming separation steps and reduce disposal needs for corrosive liquids, which makes our process more environmentally friendly and energy-saving. It is well known that crude glycerol from biodiesel production contains water unavoidably and water is also a product of the reaction sequence, which makes water the desired solvent for glycerol hydrogenolysis from the standpoint of environmental and economical viability. In this work, we reported a detailed study of continuous hydrogenolysis of glycerol over Pt-HSiW/SiO_2 bi-functional catalysts in aqueous medium. We examined the effects of HSiW content, reaction temperature, hydrogen pressure, weight hourly space velocity (WHSV) on the catalytic performance. Furthermore, a comparison between the performance of Cu-HSiW/SiO_2 and Pt-HSiW/SiO_2 under identical conditions was presented later.

2 Experimental

2.1 Catalyst Preparation

The Pt/SiO_2 catalysts were prepared by impregnation of silica support (Qingdao Haiyang Chemical Co., Ltd, 20–40 mesh, 374 m^2/g) with an aqueous solution $H_2PtCl_6{\cdot}6H_2O$ (AR, SCRC). Impregnated samples were dried overnight at 110 °C and then calcined in static air at 400 °C for 4 h. The Pt-HSiW/SiO_2 catalysts were prepared by impregnation of Pt/SiO_2 catalysts with aqueous solutions containing the desired amount of HSiW (AR, SCRC). After impregnation, samples were dried overnight at 110 °C and then calcined in static air at 350 °C for 4 h. The actual HSiW and Pt loadings were evaluated by ICP. The difference between nominal and measured mass ratio is minor. Thus the samples are hereafter referred by their nominal compositions. The catalysts are generally labeled as Pt-xHSiW/SiO_2, in which x stands for the nominal weight loading of HSiW. The loading of Pt were fixed at 2 wt% in all catalysts. Additionally, 10Cu-15HSiW/SiO_2 was prepared as a reference sample according to the method described previously [31].

2.2 Catalyst Characterization

N_2 adsorption–desorption isotherms were recorded at −196 °C on a Micromeritics ASAP 2420 instrument. Prior to the measurement, each sample was degassed under vacuum at 300 °C for 8 h.

Powder X-ray diffraction (XRD) patterns were recorded on a D2/max-RA X-ray diffractometer (Bruker, Germany), using Cu Kα radiation at 30 kV and 10 mA. The X-ray patterns were recorded in 2θ values ranging from 7° to 80°.

CO chemisorption was carried out in Auto Chem.II2920 equipment (Mircromeritics, USA). In a typical run, about 0.2 g sample was filled in a U-shaped quartz tube. The sample was first reduced by H_2 at 300 °C for 2 h, flushed with He at the same temperature for 1 h and then cooled down to 50 °C. The CO chemisorption was operated by pulse injection of pure CO at 50 °C. The Pt particle size was calculated by assuming an adsorption of one CO molecule per surface platinum atom.

NH_3-TPD was carried out in the same apparatus as above. In a typical experiment about 0.2 g sample was loaded in a U-shaped quartz tube. Prior to each run, the catalyst sample was pretreated in He at 350 °C for 1 h, then cooled to 100 °C and was saturated with pure NH_3 for 30 min. After being purged with He for 30 min, the sample was heated to 700 °C at a heating rate of 10 °C/min and the NH_3 desorption was monitored with a TCD detector. All the detected TPD peaks were deconvoluted at different maxima peak temperatures with a Gaussian function for

fitting, and the peak areas were calculated. The peak area can be correlated with the amount of adsorbed NH_3 on the basis of the pulsed NH_3 injection experiment.

Raman spectra were recorded with a LabRAM HR800 System equipped with a CCD detector at room temperature. The 325 nm of the He-Cd laser was used as the exciting source with a power of 30 MW.

ICP optical emission spectroscopy (Optima2100DV, PerkinElmer) was used to analyze the chemical composition of the catalysts.

IR spectra of adsorbed pyridine (Py-IR) were measured with VERTEX70 (Bruker) FT-IR spectrophotometer, equipped with a deuterium triglycine sulphate (DTGS) detector. The samples were degassed in a vacuum at 300 °C for 1 h, and then exposed to the pyridine vapor after cooling down to 30 °C. The Py-IR spectra were then recorded at 100 and 200 °C after applying vacuum for 30 min.

2.3 Catalytic Tests

The catalytic reaction of glycerol was performed in a down flow fixed-bed reactor (i.d. 12 mm, length 600 mm) with an ice-water trap. In a typical run, 4.0 g catalyst (20–40 mesh) was charged in the constant temperature section of the reactor, with quartz sand packed in both ends. Prior to the test, the catalyst sample was in situ reduced in a stream of pure H_2 (100 mL/min) at 300 °C for 2 h. After reduction, a 10 wt% glycerol aqueous solution and H_2 were fed into the reactor through a preheating zone which was maintained at 120 °C. The liquid and gas products were cooled and collected in a gas–liquid separator immersed in an ice-water trap and then three samples were obtained to collect representative dada for each set-point. Activity and product distributions calculated from the samples showed negligible differences. Total time-on-steam typically amounted to 24 h. The catalyst activity within this time period was rather stable.

The liquid products were analyzed by a gas chromatography (Ruihong chromatogram analysis Co., Ltd, China) with a flame ionization detector and a capillary column (DB-WAX, 30 m × 0.32 mm). The tail gas was off-line analyzed using a gas chromatograph (Huaai chromatogram analysis Co., Ltd, China) equipped with a column (OV-101, 60 m × 0.25 mm) and a thermal conductivity detector. The products were identified by GC–MS analysis.

The mass balances for liquid products accounted for 93–98% and the selectivity of gas products never exceeded 2%. The identified products were 1,3-PDO, 1,2-PDO, 1-propanol (1-PO), 2-propanol (2-PO), ethanol, propionaldehyde, acetone, propionic acid, acetic acid, acetol, acrolein, ethylene glycol, propane, methane, CO_2 and traces of unknown products such as cyclic acetals. The conversion of glycerol, selectivity and yield of products were calculated as follows:

$$\text{Conversion}(\%) = \frac{\text{moles of glycerol (in)} - \text{moles of glycerol (out)}}{\text{moles of glycerol (in)}} \times 100$$

$$\text{Selectivity}\ (\%) = \frac{\text{moles of one product}}{\text{moles of all liquid products}} \times 100$$

$$\text{Yield}\ (\%) = \frac{\text{moles of one product}}{\text{moles of glycerol (in)}} \times 100$$

3 Results and Discussion

3.1 Catalyst Characterization

Table 1 lists the physicochemical properties for the as-prepared samples. As can be seen, there is a decrease of

Table 1 Physicochemical properties and acidities of Pt/SiO_2 and $Pt\text{-}HSiW/SiO_2$ with different HSiW loadings

Catalysts	Surface area (m^2g^{-1})	Pore size (nm)	Pore volume (cm^3g^{-1})	Dispersion (%)		NH_3-TPD peak position (°C)	Acid amount (mmol NH_3/gcat.)	Total acidity (mmol NH_3/gcat.)
				CO chemisorption	XRD			
Pt/SiO_2	369.2	7.7	0.95	11.0	10	179	0.11 (105–281 °C)	0.11
$Pt\text{-}5HSiW/SiO_2$	353.4	7.5	0.89	13.8	12	166	0.20 (121–380 °C)	1.06
						448	0.86 (380–540 °C)	
$Pt\text{-}10HSiW/SiO_2$	333.2	8.0	0.85	15.7	14	168	0.12 (117–359 °C)	1.32
						455	1.20 (359–597 °C)	
$Pt\text{-}15HSiW/SiO_2$	323.9	7.9	0.81	19.1	–	166	0.10 (124–374 °C)	1.57
						450	1.47 (374–608 °C)	
$Pt\text{-}20HSiW/SiO_2$	279.9	7.7	0.72	14.6	–	163	0.09 (130–333 °C)	1.69
						457	1.60 (333–592 °C)	
$Pt\text{-}30HSiW/SiO_2$	266.4	8.4	0.68	9.5	–	168	0.15 (135–350 °C)	1.95
						424	1.80 (350–534 °C)	

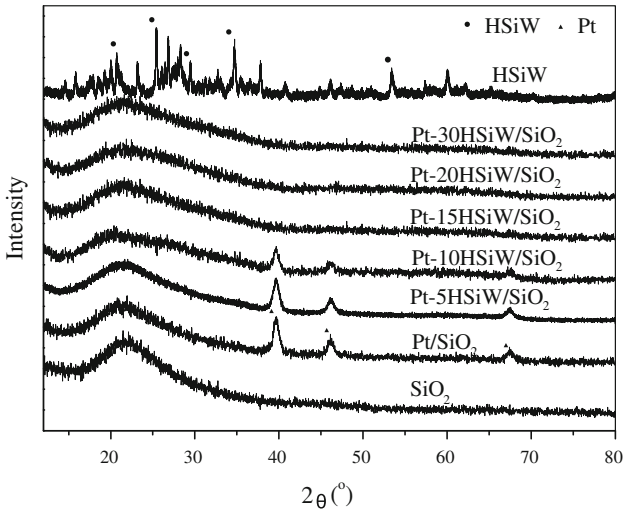

Fig. 1 XRD patterns of Pt-HSiW/SiO_2 with different loadings of HSiW

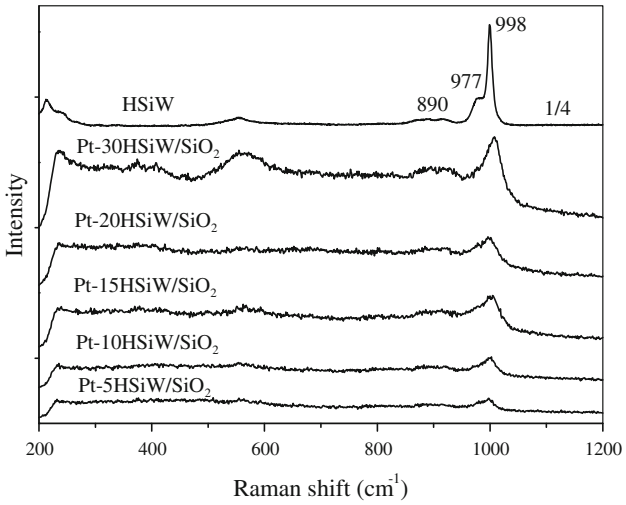

Fig. 2 Raman spectra of Pt-HSiW/SiO_2 with different loadings of HSiW

surface area and pore volume with increasing HSiW content, as previously reported over Ni-HSiW/SiO_2 [32]. This decrease is even more pronounced for Pt-30HSiW/SiO_2, perhaps due to pore blockage.

The XRD patterns of reduced Pt-HSiW/SiO_2 catalysts with different HSiW loadings are illustrated in Fig. 1. It is clear that no characteristic peak for HSiW crystallites (20.5°, 25.4°, 29.4°, 34.6°, and 53.3°) was detected for all the samples, implying the fine dispersion of HSiW on the support surface. This was well consistent with previous results [32] that the diffraction peaks of HSiW appeared at HSiW content above 50% on silica. The three peaks at 39.8°, 46.2° and 67.5° are assigned to the reflection of metallic Pt [28]. The intensity of peaks became weaker with increasing HSiW loading, and then disappeared when HSiW loading were above 10%, indicating that HSiW can improve the dispersion of Pt on the support surface to some extent. As shown in Table 1, the dispersion calculated by XRD increased with the increasing HSiW loading.

The CO chemisorption on the reduced catalysts was employed to calculate dispersion of surface Pt atoms and the results are also presented in Table 1. This dispersion firstly increased to a maximum and then decreased rapidly as the HSiW loading increased. It is assumed that HSiW can promote Pt dispersion at lower HSiW content, whereas the low dispersion at higher HSiW content is because of partial covering of the surface Pt metal with HSiW. Similar phenomenon has been reported in the case of Pd-HSiW/SiO_2 [33] and Ir-ReO_x/SiO_2 [26]. This partial covering effect can decrease surface Pt active sites and affect the activity of glycerol hydrogenolysis.

Raman spectroscopy is known to be well suited for observation of Keggin structure to verify the integrity of HSiW structure [34]. The Raman spectrum gives bands at 998, 977 and 890 cm^{-1} which are assigned to W=O symmetric and asymmetric vibrations and W–O–W asymmetric stretching vibration of bulk HSiW, respectively [32]. As shown in Fig. 2, these peaks shown up and the intensity increased with the increasing of HSiW content, confirming the presence of Keggin structure in the as-prepared samples. Compared to bulk HSiW, the slight shifts in the peaks could be attributed to the interaction of HSiW with silica support.

It has been suggested that appropriate acidity is essential for the selective hydrogenolysis of glycerol to 1,3-PDO due to the bi-functional process [14, 16, 17, 20, 35]. 1,3-PDO cannot be formed selectively over those supported metal catalysts such as Pt/C and Rh/SiO_2 without the presence of an effective acidic component. Thus, the acidic properties of the as-prepared samples were examined by NH_3-TPD and Py-IR. The strength of acid sites as determined by the NH_3 desorption temperature is generally classified as three types, weak (150–300 °C), medium (300–500 °C), and strong (500–650 °C) [34]. In Fig. 3, a small peak around 179 °C was observed over Pt/SiO_2, indicating that Pt/SiO_2 only had weak strength acid sites. In contrast, Pt-HSiW/SiO_2 showed much larger peaks at around 170 and 450 °C, indicating that it has more acidic sites with weak and medium acid strength. As shown in Table 1, the acid amount of medium acid sites was much higher than that of weak acid sites, suggesting that more medium acid sites were formed due to addition HSiW to Pt/SiO_2. The amount of acid sites increased gradually with increasing HSiW content.

Py-IR spectra of Pt/SiO_2 and Pt-15HSiW/SiO_2 catalysts at 100 and 200 °C are displayed in Fig. 4. The bands at 1,450 and 1,540 cm^{-1} are attributed to the pyridine adsorbed on the Lewis acid and Brønsted acid sites,

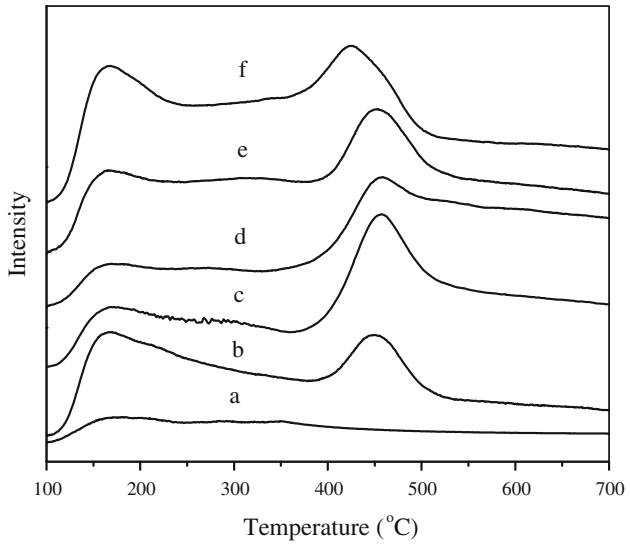

Fig. 3 NH_3-TPD profiles of **a** Pt/SiO_2; **b** $Pt\text{-}5HSiW/SiO_2$; **c** $Pt\text{-}10HSiW/SiO_2$; **d** $Pt\text{-}15HSiW/SiO_2$; **e** $Pt\text{-}20HSiW/SiO_2$; **f** $Pt\text{-}30HSiW/SiO_2$

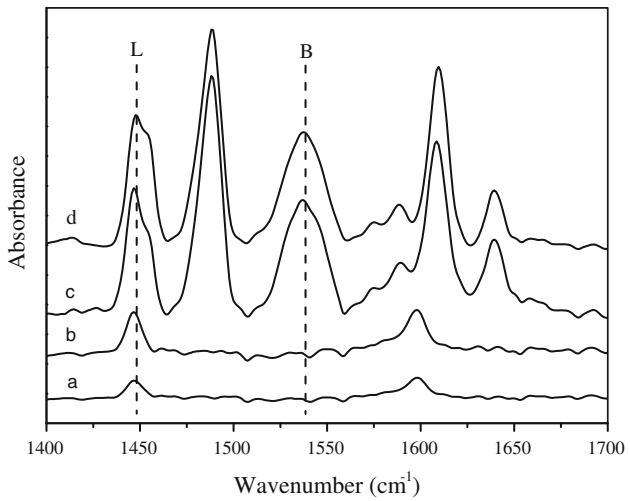

Fig. 4 Py-IR spectra of **a** 200 °C, Pt/SiO_2; **b** 100 °C, Pt/SiO_2; **c** 200 °C, $Pt\text{-}15HSiW/SiO_2$; **d** 100 °C, $Pt\text{-}15HSiW/SiO_2$

respectively [16]. The concentrations of Lewis (L) acid and Brønsted (B) acid sites are obtained from the bands at 1,450 and 1,540 cm^{-1} [36] and the calculated L/(L + B) ratios are listed in Table 2. The results show that both the amount and ratio of Brønsted acid sites increase remarkably by doping HSiW on Pt/SiO_2. Concurrently, the decrease of L/(L + B) ratios with the increase of evacuation temperature indicates that Brønsted acid sites are stronger than Lewis acid sites. Thus, HSiW is responsible for inducing the presence of Brønsted acid sites, consistent with the previous reports [32, 37].

Table 2 Amount of acid sites determined by Py-IR on Pt/SiO_2 and $Pt\text{-}15HSiW/SiO_2$

Catalysts	Acid sites (mmol/g)				L/(B + L) ratio	
	Lewis		Brønsted			
	100 °C	200 °C	100 °C	200 °C	100 °C	200 °C
Pt/SiO_2	0.0424	0.0180	0.0116	0.0112	0.79	0.62
$Pt\text{-}15HSiW/SiO_2$	0.0653	0.0571	0.1406	0.1385	0.32	0.29

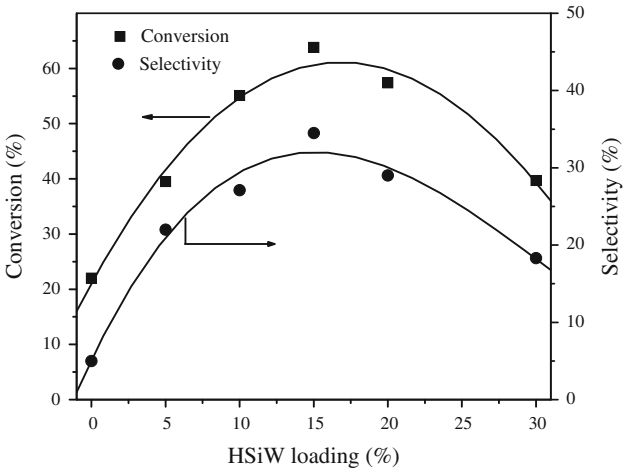

Fig. 5 Effect of HSiW loading on the conversion of glycerol and selectivity to 1,3-PDO over $Pt\text{-}HSiW/SiO_2$. Reaction conditions: 200 °C, 5.0 MPa, 4.0 g catalysts; 10 wt% glycerol aqueous solution, H_2/glycerol = 137:1 (molar ratio), WHSV = 0.045 h^{-1}

3.2 Influence of HSiW Loading

Figure 5 shows the effect of HSiW loading on glycerol hydrogenolysis over $Pt\text{-}HSiW/SiO_2$. Over the Pt/SiO_2 catalyst, the conversion and selectivity to 1,3-PDO were only 19.3 and 5.0%, respectively. Compared with Pt/SiO_2, the activity and selectivity to 1,3-PDO over $Pt\text{-}5HSiW/SiO_2$ increased sharply. With increasing HSiW content, both conversion and 1,3-PDO selectivity increased linearly, but further increase led to the decrease of activity and 1,3-PDO selectivity. The optimal loading of HSiW was 15%, in which case glycerol conversion and 1,3-PDO selectivity attained maxima: 63.8 and 34.5%, respectively. It is suggested that HSiW can affect the reactivity of glycerol hydrogenolysis significantly.

Concerning the activity of the catalysts, $Pt\text{-}15HSiW/SiO_2$ was most active, probably due to the good dispersion of Pt and suitable acidity. The CO chemisorption results suggest that the $Pt\text{-}15HSiW/SiO_2$ catalyst exhibited the highest dispersion (Table 1). On the other hand, 15 wt% HSiW loading seemed to provide sufficient acidity to

obtain high activity and further increase of HSiW loading resulted in a negative effect on the catalytic performance of the catalyst, which might be a result of the unsuitable metal/acid ratios.

Compared to Pt/SiO_2, the selectivity to 1,3-PDO over Pt-HSiW/SiO_2 enhanced remarkably. According to the literatures [38, 39], Brønsted acid sites played a key role in the dehydration of glycerol to 3-hydroxypropionaldehyde, which subsequently hydrogenated to form 1,3-PDO or further dehydrated to produce acrolein. These results lead to the proposition that Brønsted acid sites were more advantageous than Lewis acid sites for the selective hydrogenolysis of glycerol to 1,3-PDO. Thus, it is obvious that Brønsted acid sites are indispensable in order to produce 1,3-PDO selectively.

Additionally, in order to explore the role of metal Pt for glycerol hydrogenolysis, we conducted the reaction with HSiW/SiO_2 under the same condition as other catalysts. For the HSiW/SiO_2 catalyst, the conversion and selectivity to 1,3-PDO was very poor (5.8 and 3.2%, respectively) and large amounts of dehydration products such as acrolein and acetol were formed, indicating that the hydrogenation sites of Pt are also essential to form 1,3-PDO. In summary, it can be concluded that efficient catalytic reactivity in glycerol hydrogenolysis to 1,3-PDO are realized by the combination of Brønsted acid sites of HSiW and active hydrogen species of Pt.

The above results reveal that Brønsted acid sites was favorable to produce 1,3-PDO selectively. Additionally, the high loading of HSiW led to the decrease of 1,3-PDO selectivity. Thus, the balance between acidic sites and active hydrogen species played a key role in formation 1,3-PDO effectively. Since the Pt-15HSiW/SiO_2 sample exhibited the highest performance, the following investigations conducted on this sample.

3.3 Influence of Weight Hourly Space Velocity

The WHSV dependence of glycerol hydrogenolysis over Pt-15HSiW/SiO_2 is noted in Table 3. Conversion of glycerol decreased remarkably with increasing WHSV because residence time shortened correspondingly. Simultaneously, the selectivity to 1,3-PDO increased along with the decrease of 1-PO, indicating that the short residence time favored to suppress 1,3-PDO overhydrogenolysis to 1-PO.

3.4 Influence of Temperature

Figure 6 shows the effect of reaction temperature on glycerol hydrogenolysis over Pt-15HSiW/SiO_2. As expected, glycerol conversion increased monotonically from 16.3 to 99.4% with increasing temperature from 180 to 210 °C. The selectivity to 1,3-PDO dropped from 41.7% at 180 °C to 17.1% at 210 °C. In contrast, the increase of temperature positively affected 1,2-PDO selectivity, because it may be easier to activate terminal hydroxyl groups of glycerol at high temperature [28]. Concurrently, 1-PO selectivity increased linearly with the increasing temperature as high temperature facilitated to overhydrogenolysis of propanediols [30]. The optimum reaction temperature lies between 180 and 200 °C due to the high selectivity to desired 1,3-PDO with reasonable conversion.

Table 3 Influence of WHSV on glycerol hydrogenolysis over Pt-15HSiW/SiO_2

WHSV (h^{-1})	Conversion (%)	Selectivity (%)[a]				
		1,3-PDO	1,2-PDO	n-PO	i-PO	Others[b]
0.03	88.5	27.2	24.8	36.9	5.5	5.6
0.045	63.8	34.5	17.6	35.6	5.2	7.1
0.075	24.2	37.7	24.1	27.5	1.6	9.1
0.15	9.4	40.1	30.9	23.7	1.2	4.1

Reaction conditions: 200 °C, 5.0 MPa, 4.0 g catalysts; 10 wt% glycerol aqueous solution; H_2/glycerol = 137:1 (molar ratio)

[a] 1,3-PDO: 1,3-propanediol, 1,2-PDO: 1,2-propanediol, 1-PO: 1-propanol, 2-PO: 1-propanol

[b] Others include ethanol, methanol, acetone, acetol, propane, etc

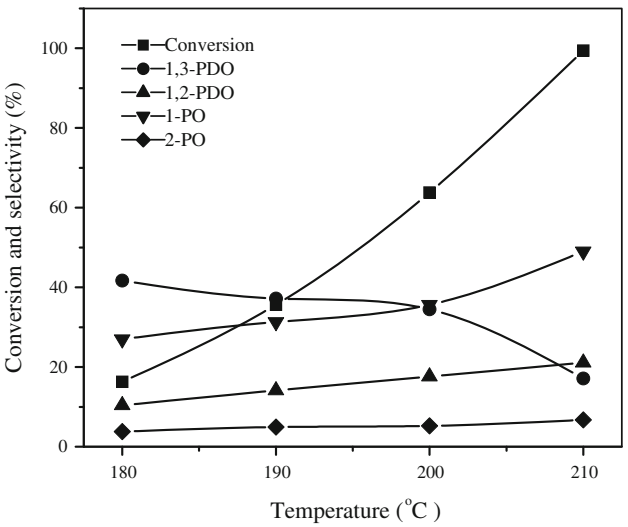

Fig. 6 Effect of reaction temperature on glycerol hydrogenolysis over Pt-15HSiW/SiO_2. Reaction conditions: 5.0 MPa, 4.0 g catalysts; 10 wt% glycerol aqueous solution, H_2/glycerol = 137:1 (molar ratio), WHSV = 0.045 h^{-1}

3.5 Influence of Hydrogen Pressure

Figure 7 shows the effect of H_2 pressure on glycerol hydrogenolysis over Pt-15HSiW/SiO_2 at 200 °C. Glycerol

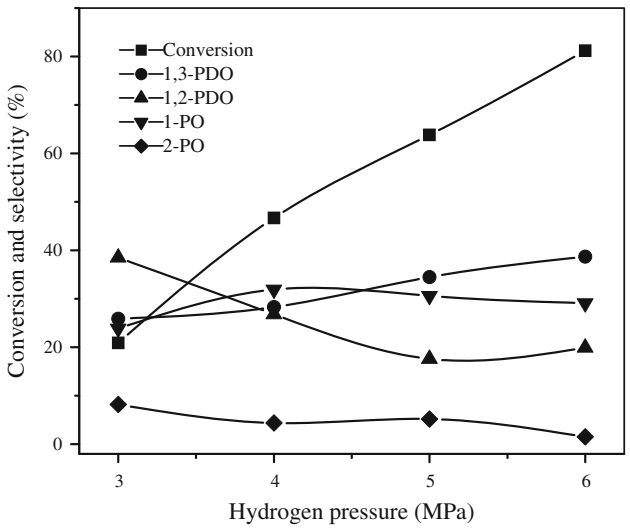

Fig. 7 Effect of H_2 pressure on glycerol hydrogenolysis over Pt-15HSiW/SiO_2. Reaction conditions: 200 °C, 4.0 g catalysts; 10 wt% glycerol aqueous solution, H_2/glycerol = 137:1 (molar ratio), WHSV = 0.045 h^{-1}

conversion improved significantly with increasing H_2 pressure from 3.0 to 6.0 MPa. The yield of 1,3-PDO increased with H_2 pressure and maximal yield of 1,3-PDO (31.4%) was achieved at 6.0 MPa and 200 °C. Concurrently, the selectivity to 1,2-PDO decreased gradually with increasing H_2 pressure except the high pressure range (>5 MPa). In summary, as reported previously [31], the increase of hydrogen pressure is favorable to form 1,3-PDO, which might be due to the increase in the active hydrogen species formed from hydrogen on Pt-15HSiW/SiO_2.

Previously we have investigated vapor-phase hydrogenolysis of glycerol to 1,3-PDO over 10Cu-15HSiW/SiO_2 [31]. Under the optimized conditions, the glycerol conversion and 1,3-PDO selectivity achieved 83.4 and 32.1%, respectively. Since the evaporation of glycerol was energy-consuming, the liquid phase catalytic process was more suitable and conducted in this article. Additionally, a comparison between the performances of 10Cu-15HSiW/SiO_2 and Pt-15HSiW/SiO_2 under identical conditions was made. Thus, hydrogenolysis of glycerol over 10Cu-15HSiW/SiO_2 was examined in aqueous-phase at 200 °C and 6.0 MPa. The conversion of glycerol and selectivity to 1,3-PDO were only 9.1 and 8.9% over 10Cu-15HSiW/SiO_2, respectively. Compared to 10Cu-15HSiW/SiO_2, the yield of Pt-15HSiW/SiO_2 increased remarkably (conversion 81.2%, 1,3-PDO selectivity 38.7%). On the other hand, in comparison with the literature [31], the great discrepancy of performance over 10Cu-15HSiW/SiO_2 was mainly due to the different hydrogenolysis process.

4 Conclusions

Our present work has demonstrated that glycerol can be effectively and selectively converted to 1,3-PDO in aqueous medium over Pt-HSiW/SiO_2 bifunctional catalysts. Brønsted acid sites with appropriate acid strength was related to form 1,3-PDO selectively. The content of HSiW affected the performance of glycerol hydrogenolysis significantly, indicating that a well balance between Brønsted acid sites and active hydrogen species is responsible for the good yield of 1,3-PDO. Finally, the conversion of glycerol and the selectivity to 1,3-PDO greatly depend on the WHSV, temperature and hydrogen pressure.

Acknowledgments The authors gratefully acknowledge the financial support of the Natural Science Foundation of China (No. 20976185). This work was also supported by the Major State Basic Research Development Program of China (973 Program) (No. 2012CB215305).

References

1. Behr A, Eilting J, Irawadi K, Leschinski J, Lindner F (2008) Green Chem 10:13
2. Huber GW, Iborra S, Corma A (2006) Chem Rev 106:4044
3. Corma A, Iborra S, Velty A (2007) Chem Rev 107:2411
4. Alonso DM, Bond JQ, Dumesic JA (2010) Green Chem 12:1493
5. Amada Y, Koso S, Nakagawa Y, Tomishige K (2010) ChemSusChem 3:728
6. Zhou CHC, Beltramini JN, Fan YX, Lu GQM (2008) Chem Soc Rev 37:527
7. Ryneveld E, Mahomed A, Heerden P, Friedrich H (2011) Catal Lett 141:958
8. Shinmi Y, Koso S, Kubota T, Nakagawa Y, Tomishige K (2009) Appl Catal B 94:318
9. Balaraju M, Rekha V, Prasad PSS, Prasad RBN, Lingaiah N (2008) Catal Lett 126:119
10. Sun J, Liu H (2011) Green Chem 13:135
11. Behr A, Eilting J, Irawadi K, Leschinski J, Lindner F (2008) Chim Oggi 26:32
12. Kraus GA (2008) Clean Soil Air Water 36:648
13. Akiyama M, Sato S, Takahashi R, Inui K, Yokota M (2009) Appl Catal A 371:60
14. Balaraju M, Rekha V, Prasad PSS, Devi BLAP, Prasad RBN, Lingaiah N (2009) Appl Catal A 354:82
15. Miyazawa T, Koso S, Kunimori K, Tomishige K (2007) Appl Catal A 329:30
16. Gandarias I, Arias PL, Requies J, Guemez MB, Fierro JLG (2010) Appl Catal B 97:248
17. Alhanash A, Kozhevnikova EF, Kozhevnikov IV (2008) Catal Lett 120:307
18. Zhao J, Yu WQ, Chen C, Miao H, Ma H, Xu J (2010) Catal Lett 134:184
19. Mane RB, Hengne AM, Ghalwadkar AA, Vijayanand S, Mohite PH, Potdar HS, Rode CV (2010) Catal Lett 135:141
20. Miyazawa T, Kusunoki Y, Kunimori K, Tomishige K (2006) J Catal 240:213
21. Huang L, Zhu YL, Zheng HY, Li YW, Zeng ZY (2008) J Chem Technol Biotechnol 83:1670
22. Vasiliadou ES, Heracleous E, Vasalos IA, Lemonidou AA (2009) Appl Catal B 92:90

23. Che TM (1987) US Patent 4,642,394, Celanese Corp
24. Chaminand J, Djakovitch L, Gallezot P, Marion P, Pinel C, Rosier C (2004) Green Chem 6:359
25. Kurosaka T, Maruyama H, Naribayashi I, Sasaki Y (2008) Catal Commun 9:1360
26. Amada Y, Shinmi Y, Koso S, Kubota T, Nakagawa Y, Tomishige K (2011) Appl Catal B 105:117
27. Nakagawa Y, Shinmi Y, Koso S, Tomishige K (2010) J Catal 272:191
28. Gong L, Lu Y, Ding Y, Lin R, Li J, Dong W, Wang T, Chen W (2010) Appl Catal A 390:119
29. Daniel OM, DeLaRiva A, Kunkes EL, Datye AK, Dumesic JA, Davis RJ (2010) ChemCatChem 2:1107
30. Qin LZ, Song MJ, Chen CL (2010) Green Chem 12:1466
31. Huang L, Zhu YL, Zheng HY, Ding GQ, Li YW (2009) Catal Lett 131:312
32. Jin H, Yi X, Sun X, Qiu B, Fang W, Weng W, Wan H (2010) Fuel 89:1953
33. Kawakami T, Ooka Y, Hattori H, Chu W, Kamiya Y, Okuhara T (2008) Appl Catal A 350:103
34. Atia H, Armbruster U, Martin A (2008) J Catal 258:71
35. Wawrzetz A, Peng B, Hrabar A, Jentys A, Lemonidou AA, Lercher JA (2010) J Catal 269:411
36. Emeis CA (1993) J Catal 141:347
37. Xu S, Wang L, Chu W, Yang W (2009) J Mol Catal A 310:138
38. Alhanash A, Kozhevnikova EF, Kozhevnikov IV (2010) Appl Catal A 378:11
39. Cavani F, Guidetti S, Marinelli L, Piccinini M, Ghedini E, Signoretto M (2010) Appl Catal B 100:197